

# Reaction of ammonia and dioxygen in solid neon excited with far-ultraviolet radiation investigated with electronic and vibrational spectra

Sheng-Lung Chou, J.F. Ogilvie, Jen-Iu Lo, Yu-Chain Peng, and Bing-Ming Cheng

**Abstract:** Irradiation of dilute mixtures of  $\text{NH}_3$  and  $\text{O}_2$  dispersed in solid Ne at 3.6 K with light of wavelengths 200, 192.5, 173, and 143 nm from a synchrotron initiated photochemical dissociation of those precursors and the production of N, NH,  $\text{NH}_2$ , O,  $\text{O}_3$ ,  $\text{HO}_2$ , NO,  $\text{NO}_2$ ,  $\text{N}_2\text{O}$ ,  $\text{H}_2\text{O}$ , HONO in both *s*-cisoid and *s*-transoid rotational isomers, and  $\text{HONO}_2$ , detected according to their spectra in mid-infrared absorption from 450 to  $4000\text{ cm}^{-1}$  and in absorption and emission from 200 to 1100 nm.

**Key words:** mid-infrared absorption spectra, visible emission spectra, visible absorption spectra, photochemistry, far-ultraviolet excitation.

**Résumé :** L'irradiation de mélanges dilués de  $\text{NH}_3$  et d' $\text{O}_2$  dispersés dans le Ne solide à 3,6 K par une lumière synchrotron de longueurs d'onde de 200, 192,5, 173 et 143 nm a entraîné la dissociation photochimique de ces précurseurs et la formation des espèces N, NH,  $\text{NH}_2$ , O,  $\text{O}_3$ ,  $\text{HO}_2$ , NO,  $\text{NO}_2$ ,  $\text{N}_2\text{O}$ ,  $\text{H}_2\text{O}$  et HONO sous les deux formes d'isomères rotationnels, scisoïde et stransoïde, ainsi que  $\text{HONO}_2$ . Ces espèces ont été détectées selon leur spectre d'absorption dans l'infrarouge moyen de 450 à  $4000\text{ cm}^{-1}$  et leurs spectres d'absorption et d'émission de 200 à 1100 nm. [Traduit par la Rédaction]

**Mots-clés :** spectres d'absorption dans l'infrarouge moyen, spectres d'émission dans le visible, spectres d'absorption dans le visible, photochimie, excitation dans l'ultraviolet lointain.

## Introduction

Many reports have appeared on the production of novel species by means of the photochemical decomposition of a suitable precursor dispersed in an inert diluent at temperatures less than 80 K.<sup>1</sup> Apart from free radicals as fragments of a dissociated precursor that are expected products if they become trapped without further reaction, some perhaps unexpected species in singlet states have been generated in this manner. As an early instance from our own experience, after the photolysis of azidosilane,  $\text{H}_3\text{SiNNN}$ , in solid Ar at 4.2 K, iminosilicon was detected through its mid-infrared spectral lines in absorption, three for HNSi and three for DNSi;<sup>2</sup> not only a force field but even its molecular structure was deduced, which was confirmed after two decades through microwave spectra of the free molecules.<sup>3</sup> As an alternative mechanism to enable spectral observations of novel stable species, a reaction between two precursors both dispersed in an inert diluent after one or the other is excited with ultraviolet light is also practicable. As an instance of such a reaction, photochemical excitation of iodomethane in the presence of  $\text{O}_2$ , both dispersed in solid Ar near 10 K, produced the first direct spectral evidence of hydrogen hypiodite;<sup>4</sup> the perturbation of the mid-

infrared spectral lines associated with the other product, methanal, relative to its spectrum in isolated conditions in solid Ar at 4.2 K<sup>5</sup> indicated the formation of a weak intermolecular complex between the two products, likely in the form of a hydrogen bond between H of HOI and O of  $\text{H}_2\text{CO}$ .

In the present work, we have investigated a system of the latter kind, involving explicitly ammonia and dioxygen, both dispersed in solid Ne at temperature 3.6 K. To initiate the reactions, we applied tunable radiation in the far-ultraviolet region provided by a synchrotron, at four wavelengths selected to excite primarily one or other of the precursor molecules. Other than the conventional mid-infrared spectra in absorption to detect and to identify the products of such a reaction, we recorded emission spectra, during photolysis, and absorption spectra, after photolysis, both throughout the near-ultraviolet, visible, and near-infrared regions from 200 to 1100 nm. The identification of the products of reaction between the precursor species was greatly aided by the knowledge of the products of photolysis of the separate species,  $\text{NH}_3$ <sup>6</sup> and  $\text{O}_2$ ,<sup>7</sup> under similar conditions of Ne dispersant and temperature. In previous work, the photolysis of  $\text{NH}_3$  and  $\text{O}_2$  in solid Ar at 4.2 K at ratios from 1:0.2:200 to 1:5:200 was implemented with radiation at 253.7 and 184.9 nm concurrently from a Hg lamp;<sup>8</sup>

Received 26 January 2021. Accepted 15 March 2021.

S.-L. Chou, J.-I. Lo,\* Y.-C. Peng,\* and B.-M. Cheng. National Synchrotron Radiation Research Centre, 101 Hsin-Ann Road, Hsinchu Science Park, Hsinchu 300, Taiwan.

J.F. Ogilvie. Escuela de Química, Universidad de Costa Rica, Ciudad Universitaria Rodrigo Facio, San Pedro de Montes de Oca, San Jose, 11501-2060, Costa Rica; Centre for Experimental and Constructive Mathematics, Department of Mathematics, Simon Fraser University, 8888 University Drive, Burnaby, BC V5A 1S6, Canada; Institute of Quantum Physics, Irkutsk National Research Technical University, 83 Lemontov Street, Irkutsk 664074, Russian Federation.

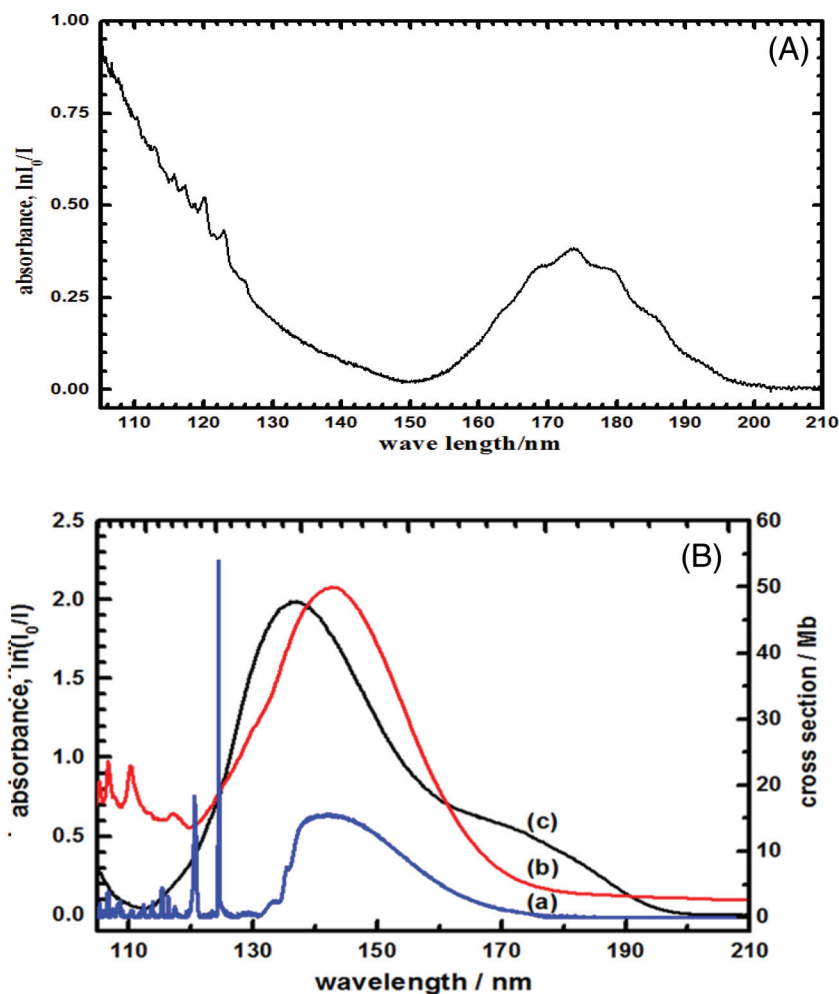
**Corresponding author:** J.F. Ogilvie (email: ogilvie@cecm.sfu.ca).

\*Present address: Department of Medical Research, Hualien Tzu Chi Hospital, Buddhist Tzu Chi Medical Foundation, No. 707, Sec. 3, Chung-Yang Rd., Hualien City 970, Taiwan.

†Present address: Tzu-Chi University of Science and Technology, No. 880, Sec. 2, Chien-Kuo Rd., Hualien City 970, Taiwan.

Copyright remains with the author(s) or their institution(s). Permission for reuse (free in most cases) can be obtained from [copyright.com](http://copyright.com).

**Fig. 1.** Absorption spectra of (A)  $\text{NH}_3$  dispersed in solid Ne, 1:500, at 3.5 K and (B)  $\text{O}_2$ , curve *b*, dispersed in solid Ne, 1:500 at 4 K, with curve *a* of gaseous  $\text{O}_2$  near 298 K and curve *c* of solid  $\text{O}_2$  at 10 K for comparison. The scale for cross section applies to only curve *a* of gaseous  $\text{O}_2$ ; the other absorbance scales are merely relative. [Colour online.]



various detected products were supposed to result from the reaction of  $\text{NH}_2$  radicals with  $\text{O}_2$ , but the speculated mechanism was based on only mid-infrared spectra with no knowledge of species such as N, O, and  $\text{N}_2$  that we prove to have a significant presence in the irradiated mixtures.

## Experiments

In these experiments, the samples were solid deposits formed from the condensation of gaseous  $\text{NH}_3$ ,  $\text{O}_2$ , and Ne in one stream onto a KBr window enclosed in a refrigerator to maintain the frozen samples at 3.6 K or a selected greater temperature; the apparatus has been described previously.<sup>6,7</sup> The capability to vary the temperature of the sample was applied for annealing operations in which, after all cycles of photolysis and respective recording of absorption spectra were completed, the temperature was increased to 8 K for 10 min and then cooled to allow the recording of further absorption spectra; raising the temperature above 8 K leads to loss of Ne from the sample. The purities of the precursors were Ne 99.9995%,  $\text{NH}_3$  99%, and  $\text{O}_2$  99.95%. The nominal ratio of components of our solid samples ( $\text{NH}_3\text{:O}_2\text{:Ne}$ ) was 1:2:1000.

These samples were subjected to irradiation with light of wavelength 200, 192.5, 173, or 143 nm selected from an undulator on beam line 21A2 of synchrotron Taiwan Light Source at National Synchrotron Radiation Research Centre. After transmission through appropriate gaseous and crystalline filters to suppress harmonics

from the undulator, the intensity of the selected light incident on our samples amounted to  $\sim 10^{15}$  photons  $\text{s}^{-1}$ , with line width  $\sim 2\%$ . Absorption spectra, in the mid-infrared range  $450\text{--}4000\text{ cm}^{-1}$  at resolution  $0.5\text{ cm}^{-1}$  and in the range  $200\text{--}1100\text{ nm}$  at resolution 0.13 or 0.26 nm, were recorded before photolysis and after sequential periods of photolysis of duration 10, 30, and 60 s, 5, 10, 30, and 30 min, and after the annealing operation. Details of the spectrometers used to record the absorption and emission spectra have been reported previously.<sup>6,7</sup> Concurrently with each period of irradiation of our samples of duration at least 60 s, emission spectra were recorded in the range  $200\text{--}1100\text{ nm}$  at spectral resolution 2.6 nm. The spectra of  $\text{NH}_3$  in Ne at 4 K and of  $\text{O}_2$  in Ne at 4 K in region  $105\text{--}210\text{ nm}$  were recorded separately at beam line 08 of Taiwan Light Source at spectral resolution 0.2 nm.

## Results

Our experiments involved photolytic excitation of our samples at four wavelengths – 200, 192.5, 173, and 143 nm. These wavelengths were selected based on the absorption spectra of  $\text{NH}_3$  dispersed in solid Ne, shown in Fig. 1a, and of  $\text{O}_2$  dispersed in solid neon, shown in Fig. 1b. The onset of absorption of  $\text{NH}_3$  in solid Ne according to electronic transition  $A^1A_2'' \leftarrow X^1A_1$  occurs at a wavelength greater than 200 nm; this absorption is significantly enhanced at 192.5 nm and attains a maximum near 173 nm, before decreasing to a perceptible minimum near 150 nm and

**Table 1.** Spectral lines of products after photolysis of  $\text{NH}_3 + \text{O}_2$  and separately  $\text{NH}_3$ <sup>6</sup> as precursor in solid Ne at 3.6 K.

Mid-infrared absorption		Absorption 200–1100 nm		Emission 200–1100 nm	
$\tilde{\nu}$ , $\text{cm}^{-1}$	Species	$\lambda$ , nm	Species, transition	$\lambda$ , nm	Species, transition
1528.4	$\text{NH}_2$ ( $\nu_2$ )	785.9	$\text{NH}_2$ , $A^2A_1 \leftarrow X^2B_1$ $\pi$ system (1, 0)	344.3	$\text{N}_2$ , $C^3\Pi_u \rightarrow B^3\Pi_g$ (0, 0)
3128.5	NH	691.6	$\text{NH}_2$ , $A^2A_1 \leftarrow X^2B_1$ $\pi$ system (2, 0)	365.9	$\text{N}_2$ , $C^3\Pi_u \rightarrow B^3\Pi_g$ (0, 1)
		624.5	$\text{NH}_2$ , $A^2A_1 \leftarrow X^2B_1$ $\pi$ system (3, 0)	390.5	$\text{N}_2$ , $C^3\Pi_u \rightarrow B^3\Pi_g$ (0, 2)
		565.4	$\text{NH}_2$ , $A^2A_1 \leftarrow X^2B_1$ $\pi$ system (4, 0)	418.1	$\text{N}_2$ , $C^3\Pi_u \rightarrow B^3\Pi_g$ (0, 3)
		512.0	$\text{NH}_2$ , $A^2A_1 \leftarrow X^2B_1$ $\pi$ system (5, 0)	449.4	$\text{N}_2$ , $C^3\Pi_u \rightarrow B^3\Pi_g$ (0, 4)
		467.9	$\text{NH}_2$ , $A^2A_1 \leftarrow X^2B_1$ $\pi$ system (6, 0)	484.8	$\text{N}_2$ , $C^3\Pi_u \rightarrow B^3\Pi_g$ (0, 5)
		429.3	$\text{NH}_2$ , $A^2A_1 \leftarrow X^2B_1$ $\pi$ system (7, 0)	525.8	$\text{N}_2$ , $C^3\Pi_u \rightarrow B^3\Pi_g$ (0, 6)
		396.2	$\text{NH}_2$ , $A^2A_1 \leftarrow X^2B_1$ $\pi$ system (8, 0)	573.3	$\text{N}_2$ , $C^3\Pi_u \rightarrow B^3\Pi_g$ (0, 7)
		367.1	$\text{NH}_2$ , $A^2A_1 \leftarrow X^2B_1$ $\pi$ system (9, 0)	335.7	NH, $A^3\Pi_1 \rightarrow X^3\Sigma^-(0, 0)$
		591.3	$\text{NH}_2$ , $A^2A_1 \leftarrow X^2B_1$ $\sigma$ system (4, 0)	799.7	NH, $a^1\Delta \rightarrow X^3\Sigma^-(0, 0)$
		535.3	$\text{NH}_2$ , $A^2A_1 \leftarrow X^2B_1$ $\sigma$ system (5, 0)	518.5	$\text{N}$ , $^2D \rightarrow ^4S$
		486.0	$\text{NH}_2$ , $A^2A_1 \leftarrow X^2B_1$ $\sigma$ system (6, 0)	324.5	Unidentified
		445.5	$\text{NH}_2$ , $A^2A_1 \leftarrow X^2B_1$ $\sigma$ system (7, 0)	464.4	Unidentified
		335.0	NH, $A^3\Pi_1 \leftarrow X^3\Sigma(0, 0)$	1011.0	Unidentified
		304.0	NH, $A^3\Pi_1 \leftarrow X^3\Sigma(1, 0)$		

Note: Numbers in parentheses after the specification of an electronic transition indicate the quantum numbers of vibrational states in the upper and lower electronic states as ( $v'$ ,  $v''$ ), respectively.

then increasing markedly in other electronic transitions toward the limit of measurements near 105 nm. In contrast,  $\text{O}_2$  in solid Ne has weak absorption at wavelengths greater than 175 nm, before an intense maximum near 143 nm, likely associated with transition  $B^3\Sigma_u^- \leftarrow X^3\Sigma_g^-$ ; spectra of gaseous and solid  $\text{O}_2$  are shown for comparison. In either case, the energy of a photon at each selected wavelength suffices to dissociate  $\text{NH}_3$  into  $\text{NH}_2 + \text{H}$  or  $\text{O}_2$  into 2 O. Although absorption by both  $\text{NH}_3$  and  $\text{O}_2$  at all selected wavelengths is likely not negligible, we assume that excitation of the dilute mixtures of  $\text{NH}_3$  and  $\text{O}_2$  dispersed in solid Ne likely involves primarily  $\text{NH}_3$  at 200, 192.5, and 173 nm and  $\text{O}_2$  at 143 nm.

The new lines assigned in absorption spectra recorded after photolysis, or in emission during photolysis, of dilute mixtures of  $\text{NH}_3$  and  $\text{O}_2$  in solid neon near 3.6 K are classified in three sets:

- lines that were previously identified<sup>6</sup> after photolysis of only  $\text{NH}_3$  in Ne (Table 1),
- lines that were previously identified<sup>7</sup> after photolysis of only  $\text{O}_2$  in Ne (Table 2),
- lines beyond those two groups that hence involve both  $\text{NH}_3$  and  $\text{O}_2$  as precursors (Table 3).

The latter lines in the mid-infrared region (Fig. 2) after photolysis at 173 nm are characteristic of OH, NO,  $\text{N}_2\text{O}$ ,  $\text{HO}_2$ ,  $\text{H}_2\text{O}$ , HONO in both *s*-cisoid and *s*-transoid rotational isomers, and  $\text{HONO}_2$ , in order of increasing molecular size.<sup>1</sup> The emission spectrum in the visible and adjacent regions (Fig. 3) during photolysis at 173 nm shows that N, O, NH, and  $\text{N}_2$  were also present and active in our samples. The absorption spectrum in the visible and adjacent regions (Fig. 4) after photolysis at 173 nm shows principally lines due to  $\text{NH}_2$  in two systems.

## Discussion

In Fig. 1b, the diffuse vibrational structure accompanying an electronic transition of  $\text{NH}_3$  in region 160–200 nm indicates that the vibrational intervals for the angular deformation  $\nu_2$  of  $\text{NH}_3$  in solid Ne are slightly larger than for the free molecule, likely resulting from a slight perturbation of this motion by the Ne lattice. In contrast, the maximum of absorption of  $\text{O}_2$  in Ne near 143 nm, according to Fig. 1a, occurs at a wavelength similar to that of the free molecule near 296 K, but appreciably greater than for pure solid  $\text{O}_2$ , 137 nm, at about the same temperature. In either case, these electronic absorption spectra provided a

**Table 2.** Spectral lines of products after photolysis of  $\text{NH}_3 + \text{O}_2$  and separately  $\text{O}_2$ <sup>7</sup> as precursor in solid Ne at 3.6 K.

Mid-infrared absorption		Emission 200–1100 nm	
$\tilde{\nu}$ , $\text{cm}^{-1}$	Species	$\lambda$ , nm	Species, transition
1039.6	$\text{O}_3$ ( $\nu_3$ )	335.7	$\text{O}_2$ , $A'^3\Delta_u \rightarrow X^3\Sigma_g^-(0, 3)$
		353.4	$\text{O}_2$ , $A'^3\Delta_u \rightarrow X^3\Sigma_g^-(0, 4)$
		372.7	$\text{O}_2$ , $A'^3\Delta_u \rightarrow X^3\Sigma_g^-(0, 5)$
		394.1	$\text{O}_2$ , $A'^3\Delta_u \rightarrow X^3\Sigma_g^-(0, 6)$
		417.6	$\text{O}_2$ , $A'^3\Delta_u \rightarrow X^3\Sigma_g^-(0, 7)$
		443.8	$\text{O}_2$ , $A'^3\Delta_u \rightarrow X^3\Sigma_g^-(0, 8)$
		472.7	$\text{O}_2$ , $A'^3\Delta_u \rightarrow X^3\Sigma_g^-(0, 9)$
		505.4	$\text{O}_2$ , $A'^3\Delta_u \rightarrow X^3\Sigma_g^-(0, 10)$
		542.1	$\text{O}_2$ , $A'^3\Delta_u \rightarrow X^3\Sigma_g^-(0, 11)$
		583.7	$\text{O}_2$ , $A'^3\Delta_u \rightarrow X^3\Sigma_g^-(0, 12)$
		631.3	$\text{O}_2$ , $A'^3\Delta_u \rightarrow X^3\Sigma_g^-(0, 13)$
		518.8	$\text{O}_2$ , $c^1\Sigma_u^- \rightarrow a^1\Delta_g(0, 4)$
		558.3	$\text{O}_2$ , $c^1\Sigma_u^- \rightarrow a^1\Delta_g(0, 5)$
		561.7	$\text{O}_2$ , $c^1\Sigma_u^- \rightarrow a^1\Delta_g(0, 6)$
		603.6	$\text{O}_2$ , $c^1\Sigma_u^- \rightarrow a^1\Delta_g(0, 7)$
		655.5	$\text{O}_2$ , $c^1\Sigma_u^- \rightarrow a^1\Delta_g(0, 8)$
		761.7	$\text{O}_2$ , $b^1\Sigma_g^+ \rightarrow X^3\Sigma_g^-(0, 0)$
		864.8	$\text{O}_2$ , $b^1\Sigma_g^+ \rightarrow X^3\Sigma_g^-(0, 1)$
		629.9	O, $^1D_2 \rightarrow ^3P_{1,2}$
		636.9	O, $^1D_2 \rightarrow ^3P_{1,2}$
		701.7	Unidentified
		750.8	Unidentified

Note: Numbers in parentheses after the specification of an electronic transition indicate the quantum numbers of vibrational states in the upper and lower electronic states as ( $v'$ ,  $v''$ ), respectively.

satisfactory basis for the design of our photolytic experiments. The presence of identified products of photolysis of  $\text{NH}_3$  and  $\text{O}_2$  indicates that absorption of light by  $\text{NH}_3$  or  $\text{O}_2$  about 200 nm sufficed to initiate photochemical reactions.

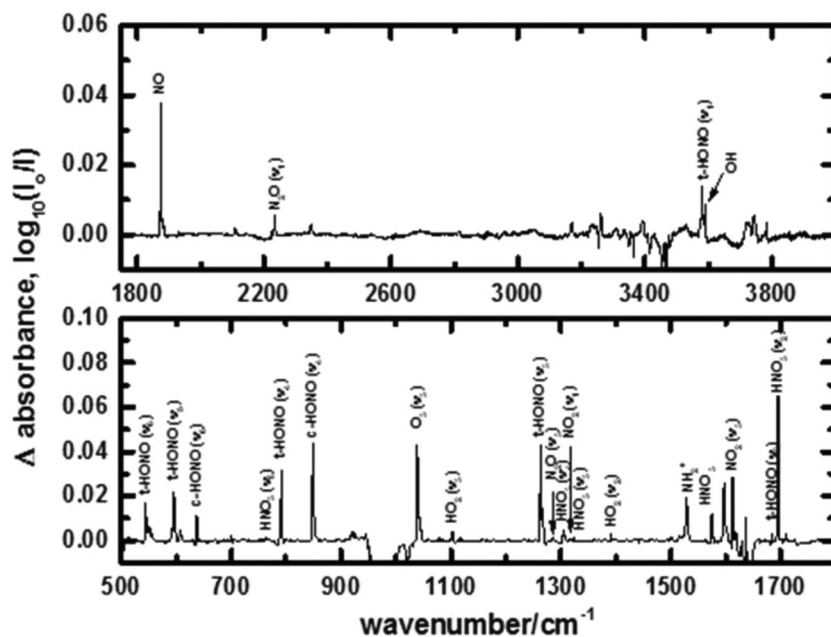
Most atomic or molecular species identified through their absorption and emission spectra have as precursor only one  $\text{NH}_3$  molecule and one  $\text{O}_2$  molecule; the exceptions to this condition are  $\text{N}_2\text{O}$ ,  $\text{O}_3$ , and  $\text{HONO}_2$ . The intensities of spectral lines are here described in relative terms. The major mid-infrared lines of  $\text{HONO}_2$  were weak after irradiation at 200 and 192.5 nm but intense at 173 nm and moderate at 143 nm. Mid-infrared lines of  $\text{O}_3$ , and  $\text{NO}_2$ , were increasingly intense as the energy of

**Table 3.** Spectral lines of products after photolysis of mixtures of NH<sub>3</sub> and O<sub>2</sub> as precursors in solid Ne at 3.6 K.

Mid-infrared absorption		Absorption 200–1100 nm		Emission 200–1100 nm	
$\tilde{\nu}$ , cm <sup>-1</sup>	Species	$\lambda$ , nm	Species, transition	$\lambda$ , nm	Species, transition <sup>a</sup>
3580.2	OH	307.2	OH A <sup>2</sup> Σ <sup>+</sup> ← X <sup>2</sup> Π <sub>i</sub> (0, 0)	307.8	OH, A <sup>2</sup> Σ <sup>+</sup> → X <sup>2</sup> Π <sub>i</sub> (0, 0)
1874.4	NO	309.1	OH A <sup>2</sup> Σ <sup>+</sup> ← X <sup>2</sup> Π <sub>i</sub> (0, 0)	309.1	OH, A <sup>2</sup> Σ <sup>+</sup> → X <sup>2</sup> Π <sub>i</sub> (0, 0)
848.5	c-HONO (ν <sub>4</sub> )	282.0	OH A <sup>2</sup> Σ <sup>+</sup> ← X <sup>2</sup> Π <sub>i</sub> (1, 0)	282.0	OH, A <sup>2</sup> Σ <sup>+</sup> → X <sup>2</sup> Π <sub>i</sub> (1, 0)
637.2	c-HONO (ν <sub>6</sub> )	283.1	OH A <sup>2</sup> Σ <sup>+</sup> ← X <sup>2</sup> Π <sub>i</sub> (1, 0)	283.1	OH, A <sup>2</sup> Σ <sup>+</sup> → X <sup>2</sup> Π <sub>i</sub> (1, 0)
3530.8	HONO <sub>2</sub> (ν <sub>1</sub> )			313.6	OH, A <sup>2</sup> Σ <sup>+</sup> → X <sup>2</sup> Π <sub>i</sub> (1, 1)
1695.0	HONO <sub>2</sub> (ν <sub>2</sub> )			314.8	OH, A <sup>2</sup> Σ <sup>+</sup> → X <sup>2</sup> Π <sub>i</sub> (1, 1)
1323.3	HONO <sub>2</sub> (ν <sub>3</sub> )			261.2	NO, A <sup>2</sup> Σ <sup>+</sup> → X <sup>2</sup> Π <sub>r</sub> (0, 3)
1305.6	HONO <sub>2</sub> (ν <sub>4</sub> )			273.9	NO, A <sup>2</sup> Σ <sup>+</sup> → X <sup>2</sup> Π <sub>r</sub> (0, 4)
763.3	HONO <sub>2</sub> (ν <sub>8</sub> )			287.7	NO, A <sup>2</sup> Σ <sup>+</sup> → X <sup>2</sup> Π <sub>r</sub> (0, 5)
1391.7	HO <sub>2</sub> (ν <sub>2</sub> )			302.6	NO, A <sup>2</sup> Σ <sup>+</sup> → X <sup>2</sup> Π <sub>r</sub> (0, 6)
1102.8	HO <sub>2</sub> (ν <sub>3</sub> )			321.7	NO, A <sup>2</sup> Σ <sup>+</sup> → X <sup>2</sup> Π <sub>r</sub> (0, 7)
2225.1	N <sub>2</sub> O (ν <sub>1</sub> )			339.1	NO, A <sup>2</sup> Σ <sup>+</sup> → X <sup>2</sup> Π <sub>r</sub> (0, 8)
1285.2	N <sub>2</sub> O (ν <sub>3</sub> )			356.5	NO, A <sup>2</sup> Σ <sup>+</sup> → X <sup>2</sup> Π <sub>r</sub> (0, 9)
1612.6	NO <sub>2</sub> (ν <sub>3</sub> )			379.1	NO, A <sup>2</sup> Σ <sup>+</sup> → X <sup>2</sup> Π <sub>r</sub> (0, 10)
3579.2	t-HONO (ν <sub>1</sub> )			264.4	NO, a <sup>4</sup> Π <sub>i</sub> → X <sup>2</sup> Π <sub>r</sub> (0, 0)
1683.8	t-HONO (ν <sub>2</sub> )			277.3	NO, a <sup>4</sup> Π <sub>i</sub> → X <sup>2</sup> Π <sub>r</sub> (0, 1)
1262.8	t-HONO (ν <sub>3</sub> )			291.0	NO, a <sup>4</sup> Π <sub>i</sub> → X <sup>2</sup> Π <sub>r</sub> (0, 2)
791.1	t-HONO (ν <sub>4</sub> )			306.5	NO, a <sup>4</sup> Π <sub>i</sub> → X <sup>2</sup> Π <sub>r</sub> (0, 3)
595.8	t-HONO (ν <sub>5</sub> )			324.5	NO, a <sup>4</sup> Π <sub>i</sub> → X <sup>2</sup> Π <sub>r</sub> (0, 4)
544.2	t-HONO (ν <sub>6</sub> )			217.7	NO, B <sup>2</sup> Π <sub>r</sub> → X <sup>2</sup> Π <sub>r</sub> (0, 1)
				226.7	NO, B <sup>2</sup> Π <sub>r</sub> → X <sup>2</sup> Π <sub>r</sub> (0, 2)
				236.5	NO, B <sup>2</sup> Π <sub>r</sub> → X <sup>2</sup> Π <sub>r</sub> (0, 3)
				246.8	NO, B <sup>2</sup> Π <sub>r</sub> → X <sup>2</sup> Π <sub>r</sub> (0, 4)
				213.5	NO, b <sup>4</sup> Σ <sup>-</sup> → X <sup>2</sup> Π <sub>r</sub> (0, 1)
				222.3	NO, b <sup>4</sup> Σ <sup>-</sup> → X <sup>2</sup> Π <sub>r</sub> (0, 2)
				232.0	NO, b <sup>4</sup> Σ <sup>-</sup> → X <sup>2</sup> Π <sub>r</sub> (0, 3)
				242.1	NO, b <sup>4</sup> Σ <sup>-</sup> → X <sup>2</sup> Π <sub>r</sub> (0, 4)
				252.9	NO, b <sup>4</sup> Σ <sup>-</sup> → X <sup>2</sup> Π <sub>r</sub> (0, 5)

**Note:** Numbers in parentheses after the specification of an electronic transition indicate the quantum numbers of vibrational states in the upper and lower electronic states as (v', v''), respectively.

<sup>a</sup>Unidentified: 270.0, 275.6, 287.7, 296.7, 305.6, 358.1, 377.5, 379.1, 427.8, 456.5, 524.3, 527.8, 548.8, 555.2, 564.5, 582.4, 612.1, 614.1, 639.1, 650.4, 679.6, 698.0, 708.5, 714.4, 718.1, 728.5, 757.6, 776.2, 915.6, 926.3, 930.4, and 1035.8 nm.

**Fig. 2.** Mid-infrared absorption spectrum after photolysis of NH<sub>3</sub> and O<sub>2</sub> in Ne at 173 nm. The curve represents the difference of absorption between after and before photolysis for 76 min; some products are identified.

**Fig. 3.** Absorption spectrum in near-ultraviolet, visible, and near-infrared regions after photolysis at 173 nm of  $\text{NH}_3$  and  $\text{O}_2$  in solid Ne at 3.6 K; some products are identified.

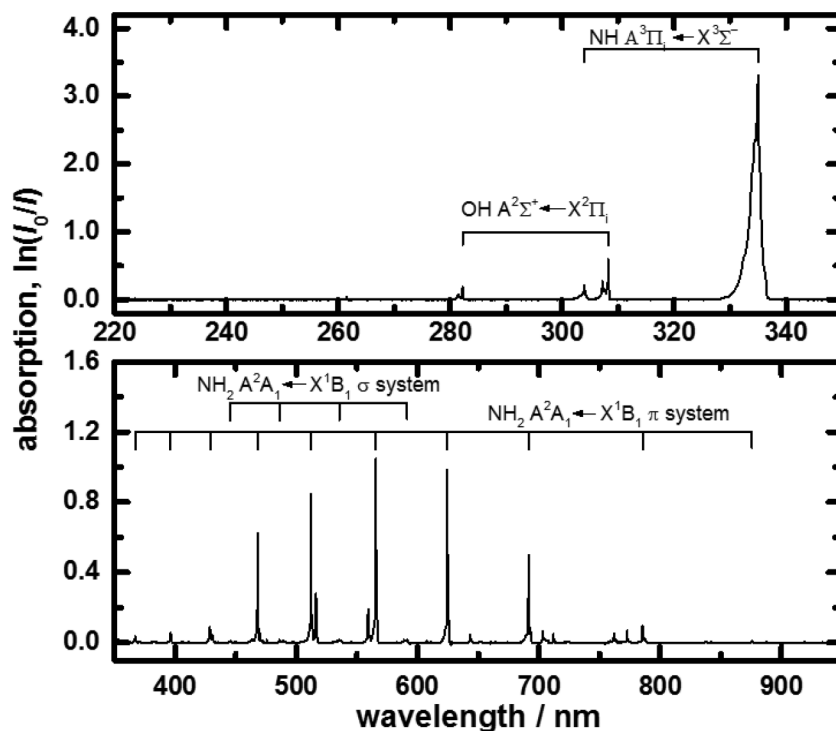
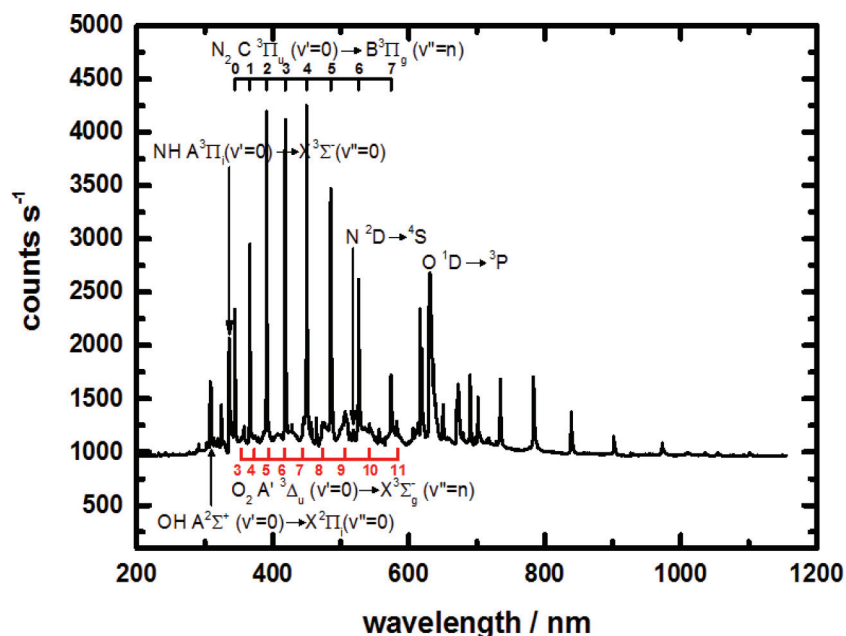


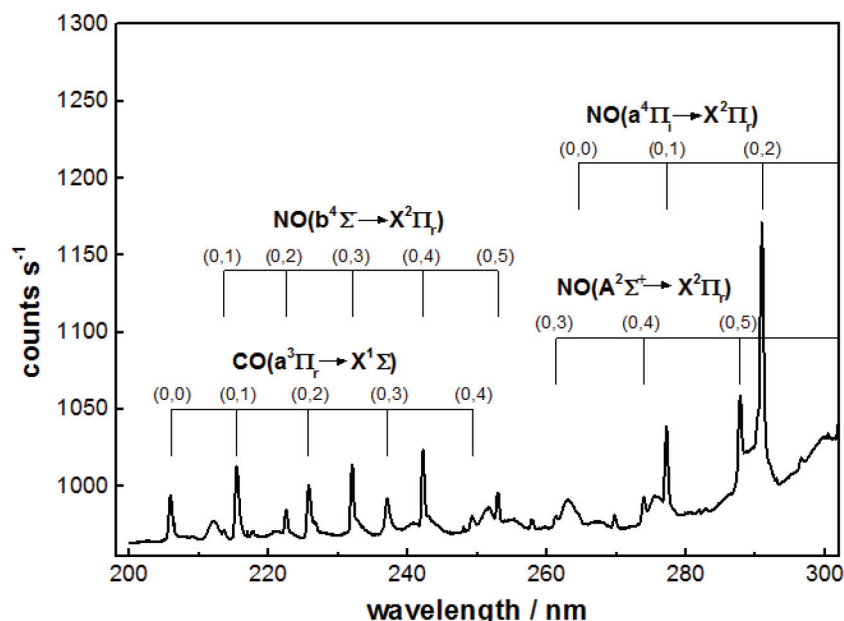
**Fig. 4.** Emission spectrum in near-ultraviolet, visible, and near-infrared regions during photolysis at 173 nm of  $\text{NH}_3$  and  $\text{O}_2$  in solid Ne at 3.6 K. Some emitters are identified. Some lines of the progression of  $\text{N}_2$  appear in the second order of the grating in region 600–1000 nm. [Colour online.]



photolytic photons increased, but lines of  $\text{N}_2\text{O}$  were weak at all photolytic wavelengths. Mid-infrared lines<sup>9</sup> of HONO in both *s*-cisoid and *s*-transoid rotational isomers were weak after photolysis at 200 and 192.5 nm, intense at 173 nm, but only moderate at 143 nm; although secondary photolysis under the latter condition is suspected, corroborating evidence is lacking as the

electronic spectra of these rotational isomers are undocumented in the far-ultraviolet region. The ratio of intensities of lines at  $791.1\text{ cm}^{-1}$  due to the *s*-cisoid rotamer and at  $848\text{ cm}^{-1}$  due to the *s*-transoid rotamer was essentially constant at all wavelengths of irradiation and at all periods of progressive photolysis from 10 s to 76 min in total.

**Fig. 5.** Emission spectrum in range 200–300 nm during photolysis at 143 nm of  $\text{NH}_3$  and  $\text{O}_2$  in solid Ne, 1:2:1000, at 3.6 K progressions of CO and NO are indicated.



Apart from other aspects, the emission spectra prove the direct involvement of atomic N and O in the reaction system, through their emission lines at 518.5 nm and 629.9, 636.9 nm, respectively, that were discernible after irradiation at 192.5 nm or smaller wavelength. The presence also of atomic H, not detected directly from any spectral line although it must arise from the primary photolytic dissociation of  $\text{NH}_3$  to  $\text{NH}_2 + \text{H}$ , is confirmed through the increased intensity of lines of  $\text{HO}_2$  after annealing: this operation, which consisted of increasing the temperature of the sample from 3.6 K to  $\sim 8$  K, maintaining that temperature for 10 min, and then recoiling to 3.6 K before recording further spectra, allowed H atoms, trapped or isolated in the Ne lattice after dissociation from  $\text{NH}_3$ , to migrate somewhat, and thus to react with available  $\text{O}_2$  molecules to form  $\text{HO}_2$ ; for this reaction, no barrier exists. A continuous absorption in the near-ultraviolet region with a maximum near 260 nm seems to increase at a rate similar to the mid-infrared lines of  $\text{HO}_2$  near 1103 and 1392  $\text{cm}^{-1}$ ; such a continuum was observed during early flash-photolysis experiments involving gaseous mixtures of  $\text{H}_2$  and  $\text{O}_2$  (R.G.W. Norrish, personal communication to JFO), but the continuous nature of that near-ultraviolet absorption precluded then, and now, a definitive assignment. In other cases, the absorption lines of  $\text{NH}_2$  in both visible and mid-infrared regions confirm definitively their assignments; for NH, only the near-infrared and near-ultraviolet lines had significant intensity, although a weak line of NH was perceptible at 3128.5  $\text{cm}^{-1}$  after irradiation at 192.5 nm. After irradiation at only 143 nm, the emission spectra also showed a progression for CO  $a^3\Pi_r, v=0 \rightarrow X^1\Sigma^+, v=0-4$ ; this CO resulted from the photolysis of  $\text{CO}_2$  present as a trace adventitious impurity during deposition (which, like  $\text{H}_2\text{O}$ , was adsorbed on surfaces of tubing leading to the cryostat and was carried with the depositing sample but was barely detectable immediately after deposition), which became dissociated to CO with radiation of wavelength 173 or 143 nm; the mid-infrared absorption spectrum concurrently exhibited a decreased absorption at 2348.7  $\text{cm}^{-1}$  due to reactant  $\text{CO}_2$  and a new line at 2141.1  $\text{cm}^{-1}$  due to product CO.

The most notable differences between experiments with photolysis at 200 nm and those at 143 nm appear in the emission spectra. At 200 nm, there are fewer emitting species, only OH,  $\text{O}_2$ ,  $\text{N}_2$ , and barely perceptible NO, and hence fewer emission lines;

their maximum intensities are of order a few hundred counts per second. In contrast, at 143 nm, there are many species and lines and their maximum intensities are of order a few thousand counts per second under the same conditions of collection; Fig. 5 shows a section of the near-ultraviolet emission spectrum from 200 to 300 nm to illustrate these effects. At 143 and 173 nm, emission lines of atomic N at 518.5 nm and of atomic O at 630 nm are prominent, whereas emission of NH near 335.7 nm and OH near 308 nm occurred at all wavelengths of excitation. The intensities of features of emission spectra from experiments with irradiation at 192.5 and 173 nm are generally intermediate between those of spectra recorded at 200 and 143 nm.

For OH formed in part as a result of reaction of H from  $\text{NH}_3$  with  $\text{O}_3$  or  $\text{N}_2\text{O}$ , not only lines 0,0 of electronic transition  $A^2\Sigma^+ \rightarrow X^2\Pi_i$  with no accompanying vibrational excitation were observed in emission at 307.8 and 309.1 nm, but also lines 1,0 at 282.0 and 283.1 nm, and even lines 1,1 at 313.6 and 314.8 nm, during irradiation at 200 nm for instance. Apart from OH, most emission lines assigned during irradiation at 200 nm correspond to transitions of  $\text{O}_2$ ,  $A^1\Sigma^+ \nu=0 \rightarrow X^3\Sigma_g^- \nu=8-13$ , and  $\text{N}_2$ ,  $C^3\Pi_u, v=0 \rightarrow B^3\Pi_g, v=0-7$ ; in the latter instance, the transition occurred between two electronically excited states of  $\text{N}_2$ , the energy of each of which is greater than that of a photon at 200 nm. A combination of a N atom in ground state  $^4S$  and another N atom in excited state  $^2P$  can result in a  $\text{N}_2$  molecule in state  $C^3\Pi_u$ , which can accordingly emit light in an intense transition to state  $B^3\Pi_g$ . The same emissions occurred after excitation at 143 nm, but their counting rates (intensities) were thousands of times as great. In addition to that transition of  $\text{N}_2$ , transition  $C^3\Pi_u, v=0 \rightarrow B^3\Pi_g, v=0-7$  was recorded after excitation at 143 nm.

The nature of the mechanism of emission of many lines in electronic transitions in these photochemical experiments is mysterious. Two well defined and pertinent mechanisms would be photoluminescence (absorption of a photon at the wavelength of irradiation and subsequent emission at the same or greater wavelength) and chemiluminescence (emission of a photon from an electronically excited molecule formed as a product of combination of atoms or free radicals). The transitions of CO,  $a^3\Pi_r \rightarrow X^1\Sigma^+$ , arise likely from the former mechanism after absorption into state  $A^1\Pi$  near 143 nm and radiationless relaxation into

state a  $^3\Pi_1$ ; the transitions of  $N_2$ ,  $C\ ^3\Pi_u \rightarrow B\ ^3\Pi_g$ , might result from the latter mechanism, but the production of N atoms in states  $^4S$  and  $^2P$  to enable that transition is not readily accounted. In other cases, neither mechanism seems applicable; radiation beyond the nominal width of the excitation lines at the selected wavelengths was perhaps not negligible.

In the absorption spectrum from 200 to 1100 nm, the most obvious features were two progressions of lines of  $NH_2$  in transitions  $A\ ^2A_1 \leftarrow X\ ^2B_1$  in both  $\pi$  and  $\sigma$  systems,<sup>6</sup> the latter of much less intensity than the former. Lines of OH were also present for the transition  $A\ ^2\Sigma^+ \leftarrow X\ ^2\Pi_1$  for both 0,0 and 1,0 features, similarly to the emission spectrum as stated above. A continuum generated with maximum near 600 nm might be due to  $O_3$  in the Chappuis bands, but again, a continuum is difficult to assign.

Our experiments with  $NH_3$  and  $O_2$  in solid Ne were conducted at relative concentrations much smaller than the preceding experiments in solid Ar.<sup>8</sup> In the latter work, the wavelength of light effective for photolysis was only 184.9 nm because absorption of precursors at 254.6 nm would be negligible. That wavelength 184.9 nm lies midway between two wavelengths, 192.5 and 173 nm, applied for excitation in our experiments. The identification of product  $NH_2OH$  in that work was apparently based on only one absorption line, at  $1118.6\text{ cm}^{-1}$ , which appears weakly also at  $1117.1\text{ cm}^{-1}$  after our irradiation at each wavelength, but our identification of  $HONO_2$  as a product not previously reported<sup>8</sup> is based definitively on five absorption lines,<sup>10</sup> at  $3530.8$ ,  $1695.0$ ,  $1323.3$ ,  $1305.4$ , and  $705.3\text{ cm}^{-1}$ , despite a smaller proportion of  $O_2$  and larger proportion of Ne.

The species detected through their various spectra as our likely products of primary photochemical reactions were also subject to secondary photolytic decomposition. For instance, a species conspicuous by its absence was  $HNO$ ; as atomic H and NO were certainly available and as their reaction lacks a significant barrier, a reason for its absence might well have been its decomposition before its proportion in a steady state was sufficient for detection, which is consistent with its known diffuse and intense absorption in region  $< 208\text{ nm}$ .<sup>11</sup> NO was detected in both mid-infrared absorption spectra and near-ultraviolet emission after irradiation at all wavelengths.

## Conclusion

Products N, NH,  $NH_2$ , O,  $O_3$ ,  $HO_2$ , NO,  $NO_2$ ,  $N_2O$ ,  $H_2O$ , HONO in both *s-cisoid* and *s-transoid* rotational isomers, and  $HONO_2$  of

reactions initiated with irradiation at 200, 192.5, 173, and 143 nm of mixtures of  $NH_3$  and  $O_2$  dispersed in proportions 1:2:1000 in solid Ne at 3.6 K were identified by means of their various spectra in absorption both in the mid-infrared region and from 200 to 1100 nm and in emission from 200 to 1100 nm. When one takes into account the greater energy of photons at 143 nm and the intensities of absorption at that wavelength, there is little evidence, according to our experiments, of a selective effect of the wavelength of irradiation on the nature of the distribution of the products generated from  $NH_3$  and  $O_2$  excited under constant other conditions.

## Declaration of interest

The authors declare that they have no known competing financial interest or personal relation that could have appeared to influence the work reported in this paper.

## Acknowledgement

Taiwan Ministry of Science and Technology (grant MOST105-2113-M-213-004-MY3) and NSRRC provided support for this research.

## References

- (1) Jacox, M. E. *Chem. Phys.* **1994**, 189, 149. doi:10.1016/0301-0104(94)00143-X.
- (2) Ogilvie, J. F.; Craddock, S. *Chem. Commun.* **1966**, 12, 364. doi:10.1039/C19660000364.
- (3) Boge, M.; Demunck, C.; Destombes, J. L.; Walters, A. *Astron. Astrophys.* **1991**, 244, L47.
- (4) Ogilvie, J. F.; Salares, V. R.; Newlands, M. J. *Can. J. Chem.* **1975**, 53, 269. doi:10.1139/v75-037.
- (5) Harvey, K. B.; Ogilvie, J. F. *Can. J. Chem.* **1962**, 40, 85. doi:10.1139/v62-014.
- (6) Chou, S.-L.; Lo, J.-I.; Peng, Y.-C.; Lu, H.-C.; Cheng, B.-M. *ACS Omega*, **2019**, 4, 2268 and references therein doi:10.1021/acsomega.8b03344.
- (7) Lo, J.-I.; Chou, S.-L.; Peng, Y.-C.; Lu, H.-C.; Ogilvie, J. F.; Cheng, B.-M. *Phys. Chem. Chem. Phys.* **2018**, 20, 13113 and references therein doi:10.1039/C8CP01375F.
- (8) Crowley, J. N.; Sodeau, J. R. *J. Phys. Chem.* **1989**, 93, 4785 and references therein doi:10.1021/j100349a021.
- (9) McDonald, P. A.; Shirk, J. S. *J. Chem. Phys.* **1982**, 77, 2355. doi:10.1063/1.444156.
- (10) Cheng, B.-M.; Lee, J.-W.; Lee, Y.-P. *J. Phys. Chem.* **1991**, 95, 2814. doi:10.1021/j100160a034.
- (11) Callear, P. M.; Wood, A. B. *Trans. Faraday Soc.* **1971**, 67, 3399. doi:10.1039/TF9716703399.